Proceedings of the ASME 2011 9th International Conference on Nanochannels, Microchannels, and Minichannels
ICNMM2011
June 19-22, 2011, Edmonton, Alberta, CANADA

ICNMM2011-58140

FLUID MECHANICS OF FLOW THROUGH RECTANGULAR HYDROPHOBIC MICROCHANNELS

Navid Kashaninejad
PhD Student
Nanyang Technological University, Singapore
navi0002@ntu.edu.sg

Weng Kong Chan
Associate Professor
Nanyang Technological University, Singapore
mwkchan@ntu.edu.sg

Nam-Trung Nguyen
Associate Professor
Nanyang Technological University, Singapore
mntnguyen@ntu.edu.sg

ABSTRACT

In this study, the effect of two important parameters have been evaluated for pressure driven liquid flows in microchannel in laminar regime by analytical modeling, followed by experimental measurement. These parameters are wettability conditions of microchannel surfaces and aspect ratio of rectangular microchannels. For small values of aspect ratio, the channel was considered to have a rectangular cross-section, instead of being two parallel plates. Novel expressions for these kinds of channels were derived using eigenfunction expansion method. The obtained two-dimensional solutions based on dual finite series were then extended to the case of a constant slip velocity at the bottom wall. In addition, for large values of aspect ratio, a general equation was obtained which is capable of accounting for different values of slip lengths for both upper and lower channel walls. Firstly, it was found out that for low aspect ratio microchannels, the results obtained by analytical rectangular 2-D model agree well with the experimental measurements as compared to one dimensional solution. For high aspect ratio microchannels, both models predict the same trend. This finding indicates that using the conventional 1-D solution may not be accurate for the channels where the width is of the same order as the height. Secondly, experimental results showed that up to 2.5% and 16% drag reduction can be achieved for 1000 and 250 micron channel height, respectively. It can be concluded that increasing the surface wettability can reduce the pressure drop in laminar regime and the effect is more pronounced by decreasing the channel height.

NOMENCLATURE

Roman Letters
b = slip length of liquids
C_1, C_2 = constants of integration
f = Darcy friction factor
g = standard gravity
H = channel height
h = half of the channel height
P = pressure
Po = Poiseuille number
Q = flow rate
u, v = velocity distribution
U = average velocity
W = channel width

Greek Letters
α = aspect ratio
β = dimensionless slip
μ = viscosity
ρ = density
Γ = perimeter of the channel

Subscripts/Superscripts
s: slip
w : wall
+: upper
- : lower
*: dimensionless

Abbreviations
B: bare
BC: boundary condition
CA: contact angle
P: PMMA
R: rectangular
SH: superhydrophobic
T: textile
Re: Reynolds number

INTRODUCTION

Since both natural systems such as blood vessels, brain, lungs and artificial ones such as heat exchangers, devices designed for chemical analysis, etc. depend on channels to fulfill their duties, investigation of fluid flow characteristics in these channels is of paramount [1] and has been dealt with scientifically since 17th century. Mostly inspired by and begun with silicon-based, however, new research fields such as Micro-Electro-Mechanical-Systems (MEMS) as well as Microfluidics, were introduced in the 1980s and 1990s, respectively [2]. Since then, unique characteristics and phenomena occurring exclusively in the miniaturized domain were reported.
Incorporating polymeric materials such as poly-methylmetacrylate (PMMA) and poly-dimethylsiloxane (PDMS) beside silicon and glass, facilitates the micro-domain fabrication techniques tremendously. Nevertheless, theoretical models describing small scale phenomena have not progressed as rapidly as fabrication techniques. Fundamental hypotheses which conventional theories are based on, need to be reconsidered carefully for small scale domains, as unacceptable deviations from experimental results would occur.

Additionally, the increasing use of microchannels makes them almost indispensible in some fields such as inkjet technology, drug delivery, Lab-on-a-chip devices and genetic research area. However, the field of microfluidics has its own limitations, hence, devising novel ways to improve its performance is of immense importance. Surprisingly high pressure drop along the developed length of microchannels is one of these challenges. One of the recent novel methods to overcome the high frictional resistance of flow in small scale domains is to enhance the slip boundary conditions on the channel walls. Study of slip in liquid flows not only can explain the reasons of most of the existing deviations between theoretical modeling and experimental results in microchannels, but it can also provide ideas on how to reduce the pressure drop.

Slip can be detected both directly and indirectly [3]. According to the indirect experimental observations of [4-7] which were further confirmed by direct experimental methods of [8-10], order of slip for smooth hydrophobic surfaces cannot exceed more than a few nanometers. Therefore, as the characteristic length scale of the system increases, the assumption of no-slip boundary condition becomes more accurate. To achieve larger slip, the interests have been shifted to a new generation of the surfaces known as superhydrophobic surfaces. Generally, when the static contact angle (CA) on a surface is large, for instance more than 150 degree, and its CA hysteresis is small, for instance less than 10 degree, the surface is termed superhydrophobic (SH). First observed on a lotus leaf, superhydrophobicity exists due to the presence of micro and nano-size roughness on the surface. When a droplet is deposited on such a surface, it stays atop the roughness asperities unlike the Wenzel state [11] where it penetrates into the roughness cavities. Assuming uniform roughness along the surface, air pockets can be formed beneath the droplet and theoretical CA can be calculated in this state using the Cassie-Baxter model [12]. Using the idea of implementing low energy surfaces in order to reduce the drag in laminar flows for Newtonian liquids was proposed by [13]. Surprisingly, up to 14% of drag force was reduced for water flowing in a circular pipe with a diameter in the range of several millimeters. Up to now, no other researchers have reported such extent of drag reduction with channels in that range. They attributed the efficiency of the implemented channels to the surface tension of water which prevent the liquid to penetrate into existing surface roughness. Although they did not mention any details about the surface roughness and just called them “fine groves”. Upon reducing the surface tension of the liquid (e.g., using surfactant), results were the same as non-coated smooth channel. These results were further confirmed later by [14] who fabricated different SH channels by silicon etching and then using low-surface energy coating to obtain channels with a static CA in the range of 130° up to 174° and CA hysteresis of less than 18°. They reported a slip length up to 25 μm on these SH surfaces in pressure drop versus flow rate experiment. These results showed the possibility of achieving a large slip and consequently a small pressure drop using SH microchannels in the laminar region. The height of their channels ranges from 76 to 254 micron, while the aspect ratio was very large so that the effect of side walls was neglected in the experiments.

Conflicting results reporting the effect of channel geometries as well as surface conditions, such as wettability, in pressure drop in confined channels necessitate further research in this field. In the present study, the effects of two important parameters which are usually neglected in conventional channels, namely the ratio of width over height of the channels (also known as aspect ratio) as well as wettability of the channel surface which include the roughness of the surface will be evaluated via analytical modeling followed by experimental verification.

In addition, the feasibility of implementing SH surfaces in microchannels to reduce the frictional drag in pressure driven liquid flows in laminar region will be evaluated.

ANALYTICAL MODELING

Liquid Flow in Parallel-Plate Microchannels

In previous works, it is always assumed that dominating BCs in liquid flows through microchannels are either no-slip or equal

slip conditions. In this section, the general form of Newtonian liquid flow in two parallel-plate microchannel which consists of two different walls with unequal wettability and surface condition is considered. This situation may occur frequently in microchannel fabrication, since fabricating microchannels with a single material is not always possible. In this section, it is assumed that the width of the channel is much larger than its height so that effect of side walls can be neglected. That means, a high aspect ratio microchannel is investigated. Schematic view of such microchannel is illustrated in Fig.1.

Considering fully developed laminar flow for Newtonian liquids with constant properties at low Reynolds number, the Navier-Stokes equation can be simplified to Stokes equation. Solving this ordinary differential equation, the velocity distribution in terms of BCs can be calculated as follows:

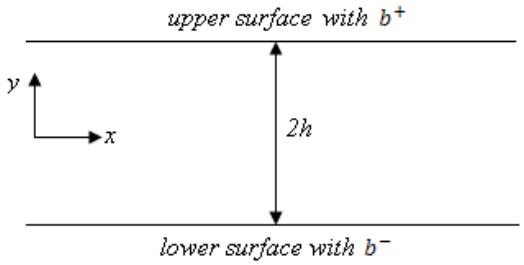

Figure 1. Schematic view of the channel with slip at both walls

$$\frac{d^2u}{dy^2} = {}^1\!/_\mu \frac{dP}{dx} \Rightarrow \frac{du}{dy} = {}^1\!/_\mu \frac{dP}{dx}\, y + C_1$$
$$\therefore u(y) = {}^1\!/_{2\mu} \frac{dP}{dx} y^2 + C_1 y + C_2 \qquad (1)$$

Corresponding Navier slip BCs at both walls are:

$$\begin{cases} u(y=+h) = -b^+ \left.\dfrac{du}{dy}\right|_{y=+h} \\ u(y=-h) = b^- \left.\dfrac{du}{dy}\right|_{y=-h} \end{cases} \qquad (2)$$

Upon imposing the BCs and further simplifications, general equation describing the velocity distribution in a non-dimensional form can be obtained as:

$$u^*(y^*) = -\frac{1}{2} y^{*2} - \frac{(\beta^- - \beta^+)}{(1+\beta^+ + \beta^-)} y^* + \frac{1}{8}\left[\frac{3\beta^+ + 3\beta^- + 8\beta^+\beta^- + 1}{\beta^+ + \beta^- + 1}\right] \qquad (3)$$

where $u^* = \frac{u}{{}^1\!/_\mu (-\frac{dP}{dx}) H^2}$, $y^* = \frac{y}{H}$, $\beta = \frac{b}{H}$

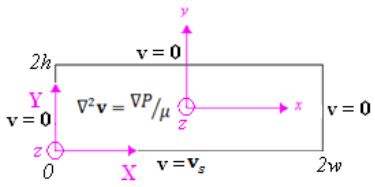

Figure 2. Rectangular microchannel with the constant slip velocity at the wall

In this case, dimensionless volumetric flow rate can also be computed as:

$$Q^* = \frac{1 + 4\beta^- + 4\beta^+ + 12\beta^+\beta^-}{12(1 + \beta^+ + \beta^-)} \qquad (4)$$

where $Q^* = \frac{Q}{{}^1\!/_\mu \left(-\frac{dP}{dx}\right) H^3 W}$

Additionally, Darcy friction factor can be calculated using the following equation:

$$f = \frac{96}{Re} \frac{\alpha^2(1+\beta^+ + \beta^-)}{(1+4\beta^- + 4\beta^+ + 12\,\beta^+\,\beta^-)(\alpha+1)^2} \qquad (5)$$

where $Re = \frac{\rho U D_h}{\mu}$, $D_h = \frac{2\alpha H}{\alpha+1}$, $\alpha = \frac{W}{H}$

Equivalently, we can also define another dimensionless number by multiplying Darcy friction factor to Reynolds number which is usually called the Poiseuille number:

$$Po = 96 \frac{\alpha^2(1+\beta^+ + \beta^-)}{(1+4\beta^- + 4\beta^+ + 12\,\beta^+\,\beta^-)(\alpha+1)^2} \qquad (6)$$

It should be noted that the aspect ratio needs to be large so that these equations can be applicable, that is:

$$W \gg H \Rightarrow \frac{W}{H} \gg 1 \rightarrow \alpha \gg 1 \qquad (7)$$

The friction factor from the above equation can only be calculated when the aspect ratio is much larger than unity. Sometimes it is completely omitted from the friction factor relation in case of two parallel-plate channels. However, it is retained here for completeness sake. In other words, the obtained formulae are valid for liquid flow through two parallel-plate microchannels not only for large aspect ratios but it can also be used to approximate relatively moderate aspect ratios.

It can be shown that by substituting $\beta^+ = \beta^- = 0$ in the Equations (3-5), the traditional equations describing velocity, flow rate and friction factor in the conventional channels, with no slip BCs, can be obtained.

Liquid Flow in Rectangular Microchannels

Although one dimensional analysis is adapted to evaluate the behavior of fluid flow in circular cross-section as well as two infinite parallel plates microchannels, analytical modeling for rectangular cross-section microchannels needs two-dimensional analysis [15]. Due to the complexity of this analysis, most of the previous research works merely focused on high aspect ratio microchannels, which in fact are channels between two parallel plates. One of the drawbacks of such analysis is that the effect of the side walls is ignored. From an experimental point of view, there might be differences between different materials used as the side walls which determine the wettability conditions and consequently affect the accuracy of measuring the slip length.

In this section, we derive expressions for the velocity and the flow rate for fluid flow in microchannels with the following assumptions:

1) The microchannel has a rectangular cross-section and a finite aspect ratio, α, which is equal to width to height ratio.

2) The length of the microchannel is sufficiently long that fully developed condition is reached and there is no variation of flow characteristics in the stream wise direction.

3) The working fluid is assumed to be incompressible and its properties remain constant.

4) The channel height is assumed to be large enough so that continuum hypothesis can be implemented correctly.

5) Pressure-driven flow is assumed, that is, the working fluid will be pumped in the streamwise direction.

According to the above-mentioned assumptions, continuity as well as Navier-Stokes equations can be used to describe the hydrodynamic behavior of the flow as follows:

$$\nabla . v = 0 \tag{8}$$

$$\rho \frac{D\mathrm{v}}{Dt} = \rho \mathrm{g} - \nabla P + \mu \nabla^2 \mathrm{v} \tag{9}$$

By neglecting the effect of gravity and assuming steady flow, the momentum equation can be simplified further. Additionally, at low Reynolds number flows, the inertia term is small, so that only the effect of viscous stress will become important which needs to be balanced by the pressure gradient.

For Re<<1 or creeping flow, the momentum equation is simplified to:

$$\nabla^2 \mathbf{v} = {}^{\nabla P}/_{\mu} \tag{10}$$

In this case, slip is assumed to exist only at the bottom plate (i.e. non symmetry case) while the three remaining walls are hydrophilic so that no-slip BC can be applied.

The domain of this type of the problem is shown in the Fig.2.

Since the governing equation is linear, we can take advantage of superposition principle and decompose the domain into two separate ones and solve each domain independently. Then by summing up each solution, the final solution of the desired domain would obtain. The procedure is shown in Fig.3:

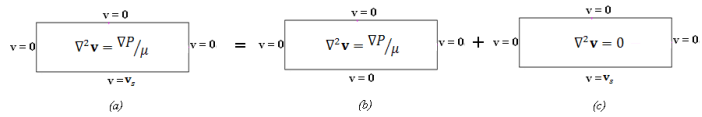

Figure 3. Required procedure for obtaining velocity distribution in a microchannel with constant velocity at bottom wall

In order to solve the first part, Fig. 3(b), the method of eigenfunction expansion can be used corresponding to homogeneous boundary conditions and non homogeneous linear governing partial differential equation (PDE) while the second part, Fig. 3(c), is the famous Laplace equation in rectangular domain with non homogeneous Drichlet boundary condition.

The velocity profile for the entire domain can be found by summing the velocity profile in each domain separately, which becomes:

$$u_{total}(x,y) = u_{No-slip} + u_{slip} \tag{11}$$

where:

$$u_{No-slip} = \frac{16\ \alpha^2 h^2}{\mu\pi^4}\left(-\frac{dP}{dz}\right)\sum_{n=1}^{\infty}\sum_{m=1}^{\infty}\frac{[1-\cos m\pi][1-\cos n\pi]}{m\,n\,(m^2+\alpha^2 n^2)}\,sin[\frac{m\pi}{2\alpha h}(x + \alpha h)]\,sin[\frac{n\pi}{2h}(y+h)]$$

and,

$$u_{slip} = \frac{2\boldsymbol{v}_s}{\pi}\sum_{k=1}^{\infty}\frac{[1-\cos k\pi]}{k\,.\,sinh\left[k\pi\frac{h}{w}\right]}sin\frac{k\pi}{2w}(x+w)\ sinh\frac{k\pi}{2w}(h-y)$$

Also, total flow rate becomes:

$$Q_{total} = Q_{No-slip} + Q_{slip} \tag{12}$$

where:

$$Q_{No-slip} = \frac{64\ h\ w^3}{\mu\pi^6}\left(-\frac{dP}{dz}\right)\sum_{n=1}^{\infty}\sum_{m=1}^{\infty}\frac{[1-\cos m\pi]^2[1-\cos n\pi]^2}{m^2\,n^2\,(m^2+\alpha^2 n^2)} \tag{12.a}$$

and,

$$Q_{slip} = \frac{4\boldsymbol{v}_s\,w}{\pi^2}\sum_{k=1}^{\infty}\frac{[1-\cos k\pi]^2}{k^2}\left[\frac{cosh\left[\frac{k\pi h}{w}\right]-1}{sinh\left[\frac{k\pi h}{w}\right]}\right] \tag{12.b}$$

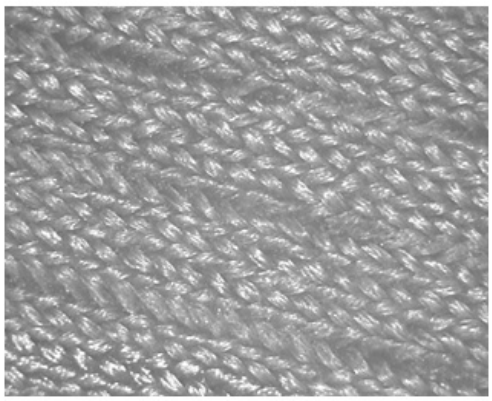

Figure 4. Optical microscopy image of Fastskin™ fabric

Rearranging, it yields the relation for slip velocity at the wall:

$$v_s = \frac{\pi^2}{4w}\frac{\left(Q_{total}-\frac{64\ h\ w^3}{\mu\pi^6}\left(-\frac{dP}{dz}\right)\sum_{n=1}^{\infty}\sum_{m=1}^{\infty}\frac{[1-cos\,m\pi]^2[1-cos\,n\pi]^2}{m^2\,n^2\,(m^2+\alpha^2n^2)}\right)}{\sum_{k=1}^{\infty}\frac{[1-cos\,k\pi]^2}{k^2}\left[\frac{cosh\left[\frac{k\pi h}{w}\right]-1}{sinh\left[\frac{k\pi h}{w}\right]}\right]} \quad (13)$$

In this section, the effect of channel aspect ratio was evaluated. In the situation where the width of the channel is of the same order as the channel height, the streamwise velocity is no longer one dimensional. Initially, it was assumed that all the four channel walls are hydrophilic so that no-slip BCs can be applied. In order to solve the equation, the method of eigenfunction expansion was used, corresponding to homogeneous boundary conditions and non homogeneous linear governing Stokes equation. The obtained solution was in terms of dual sinusoidal series, and the result agrees well with the solution of one-dimensional flow when the aspect ratio is very large. Also, instead of assuming no-slip BC at the bottom wall, flow with constant slip velocity was assumed. Using superposition principle, due to linearity of the governing Stoke equation, as well as classical method of separation of variables, the desired relationship describing velocity distribution was obtained in term of yet-unknown constant wall slip velocity. From the obtained equation, unknown slip velocity was formulated based on the total flow rate, channel height, and aspect ratio, Eq. 1)(13). By experimentally measuring the total flow rate of the channel, slip velocity can be completely calculated. To find the slip velocity in rectangular microchannels with arbitrary aspect ratio, implementing Eq. (13) will be more accurate than the previous models with one-dimensional velocity distribution. Furthermore, if the side walls of the channel are also coated with low surface energy materials and/or etched with appropriate roughness, to obtain SH surface, this approach is capable of calculating the related slip velocity.

Therefore, deviations from classical no-slip BCs are expected in microchannels of small aspect ratio and fabricated from super/hydrophobic surfaces. In order to illustrate this concept and to validate the theoretical results, experiments will be conducted with channels fabricated for different aspect ratios as well as surface wetting conditions, and the results will be compared to the corresponding analytical equations. This will be presented in the following section.

EXPERIMENTAL APPROACH

This section presents the experimental investigation of flow in microchannels. Comparison with analytical results will be presented. The effect of surface wettability (e.g., contact angle) as well as aspect ratio (width to height) on the performance of the microchannel in a pressure driven flow of liquids in laminar region (low to medium range of Reynolds number) will be investigated. The experimental test rig was devised and fabricated to measure flow rate of de-ionized (DI) water for a range of pressure difference across the rectangular cross section microchannels. The effects of different aspect ratios as well as surface conditions will also be investigated. The heights of the fabricated channels were varied from 250 μm up to 1000 μm. The test devices were fabricated in PMMA both bare and coated with hydrophobic textile.

Fabrication of Superhydrophobic Surfaces

High-water repellent surfaces have been used in textile industry more than 6 decades ago. By improving the topography and using silicon coating of commercial fabrics, surfaces with high contact angle and low rolling angle (CA hysteresis) can be obtained. However, in the literature most of the research work merely focused on very expensive, complex and in some cases time-consuming methods for fabricating superhydrophobic surfaces which can be summarized in Table 1.

Table 1. Summarizing different methods to produce micro/nano sized roughness on surfaces [16]

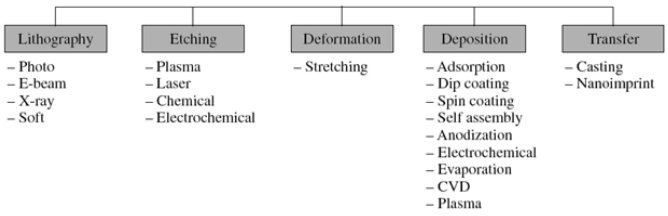

However, according to [17] modification of polyester textiles with low surface energy is probably one of the most pragmatic options to produce and fabricate superhydrophobic surfaces. In this study such commercially available fabric (Fastskin™) has been used to convert a bare PMMA surface into a superhydrophobic one.

The characteristics of such these fabrics are illustrated in Fig.4.

In this project, hydrophobized fabric was attached on PMMA and then cut to the desired dimensions. Using optical microscopy, the precise thickness of it was obtained and accordingly cut-through double sided adhesive tapes were used to compensate its excess thickness (thickness was 525 microns, hence 14 adhesive tapes with 50 micron thickness were used) and accordingly the attached hydrophobized fabric PMMA surface was become as flat as the bare PMMA surface.

Contact Angle Measurement

Wettability conditions of the fabricated surfaces were determined by FTÅ200^{TM}. The device can be used to measure the contact angle as well as other interfacial related phenomena.

Measured advancing contact angles of these surfaces are shown in Fig.5 which are $54^{\circ}, 85^{\circ}$ and 122° for bare PMMA, lotus-like PMMA and hydrophobized fabric respectively. Using casting of PDMS on lotus leaf followed by hot embossing on PMMA is capable of increasing contact angle of PMMA ($\sim 31^{\circ}$), however, the surface is still hydrophilic since the CA is slightly below 90°. Because one of the main purposes of this study is to evaluate the effect of CA on the efficiency of microchannels in pressure driven flows, fabricated microchannels were chosen from bare PMMA and attached hydrophobized fabric PMMA where CA difference was maximum.

Fabrication of Test Channels

Four channels were fabricated; two with 1000 micron height, others with 250 micron. They were cut using laser in three sheets of double-sided adhesive tapes. Thermal bonding method was also used to bond the channels, however, only the results of former are presented. To overcome leakage problems, further treatment with suitable solvent, i.e. Chloroform, was carried out.

Each dimension of the fabricated surfaces was precisely measured via optical microscopy and it was found that the uncertainty in laser cutting is at least 100 μm which is quite considerable in microchannel studies. Table 2 shows the dimensions of fabricated microchannels. The channels have been coded according to following format: (bottom-surface material)(material of whole channel)(cross-section)-(aspect ratio). For example TPR-15 refers to the channel with bottom surface coated with hydrophobized textile, fabricated completely with PMMA, its cross-section is rectangular-its aspect ratio is 15, or BPR-4 refers to the bare (untreated) bottom surface, fabricated from PMMA with rectangular cross-section whose aspect ratio is 4.

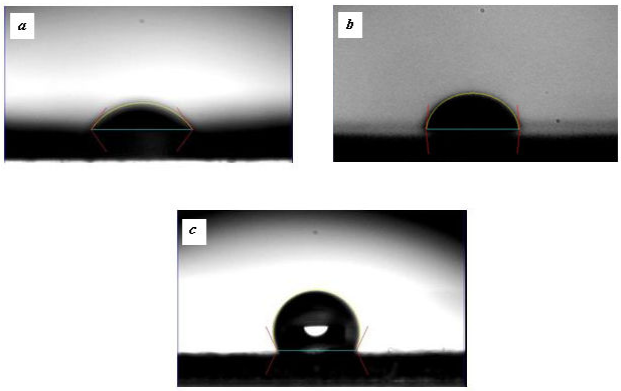

Figure 5. Measured contact angle of a) bare PMMA; b) Lotus-like PMMA; and c) hydrophobized fabric

Table 2. Detail dimensions of fabricated microchannels (T: Textile, P: PMMA, R: Rectangular, B: Bare)

Channel type	Height (**mm**)	Width (**mm**)	Length (**mm**)	Aspect ratio (**α**)
TPR-15	0.285	4.1988	57.4115	~ 15
TPR-4	1.083	4.1988	61.5129	~ 4
BPR-15	0.285	4.1988	57.4115	~ 15
BPR-4	1.083	4.1988	61.5129	~ 4

Experimental Procedure for Pressure-Driven Flow in Fabricated Microchannels

The experimental set-up consists of the following items: DI water source, Gear pumps (Cole Parmer-Variable Speed Pump Drive 75211-15), Pressure Transducer (Druck DPI 280 Series) volumetric flask & timer, connecting tubes, pressure transducer probes, and channel inlet and outlet connectors. This test rig is schematically shown in Fig.6.

To conduct the experiment, great care was taken in filling the tubes totally with DI water and air bubbles were eliminated to minimize experimental errors. Each experiment was conducted three times (on different days). To measure the flow rate, a volumetric flask beside a digital timer was used. The time needed when the flow reaches a certain prescribed volume

(say, 150 mL) was recorded several times and the average values were calculated.

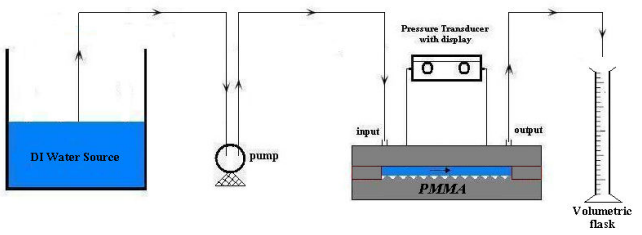

Figure 6. Schematic diagram of the conducted experiment to measure flow rate in different pressure-drop values (components are not drawn in actual scale)

RESULTS AND DISCUSSION

Wide range of pressure difference was used by adjusting the speed of the gear pump and the corresponding flow rate was measured. These results are shown in Fig.7 and Fig.8.

In the figures, comparison between theoretical modeling and experimental results was also performed. "Analytical 1-D" in figures refers to the relationship between flow rate and pressure drop in parallel-plate microchannel (where aspect ratio is large enough so that effects of side walls are negligible) and is calculated by assumption of no-slip BCs at top and bottom walls. This relation can be found via general Eq. (4) by equating both upper and lower walls slip length to zero. While "Analytical 2-D" refers to rectangular microchannel with finite aspect ratio and no-slip BCs at the walls which is calculated based on the Eq. (12.a).

The pressure drop measurements as a function of flow rate for small aspect ratio channel is shown in Fig.7. The pressure drop was found to increase linearly with flow rate. Since the channel height is large, the effect of slip is not significant. In this case, the fabricated channel can be considered as 2-D rectangular channel because the height is comparable to the width, and as expected, the obtained analytical results of 2-D rectangular channels better predict the experimental result. It is noted that for the case where the channel wall was coated with hydrophobic textile (TPR-4), at the same pressure drop the flow rate is slightly higher than the bare PMMA channel wall (BPR-4).

Figure 7 illustrates the situation where the channel height is one-fourth of the previous channel while the width remained unchanged. In this case, the aspect ratio is larger since the width is in millimeter order while the height is in micrometer. Firstly, it was found that both theoretical models predict the same trend because the aspect ratio is large and the two parallel-plate assumption is also valid. Secondly, the experimental results showed higher flow rate than the analytical ones for the same pressure drop. The reason can be attributed to the small order of the channel height. The effect of slip is more pronounced as the characteristic length of the channel shrinks. This experiment verifies this concept and also shows that slip may exist even on hydrophilic surfaces. Secondly, it is evident

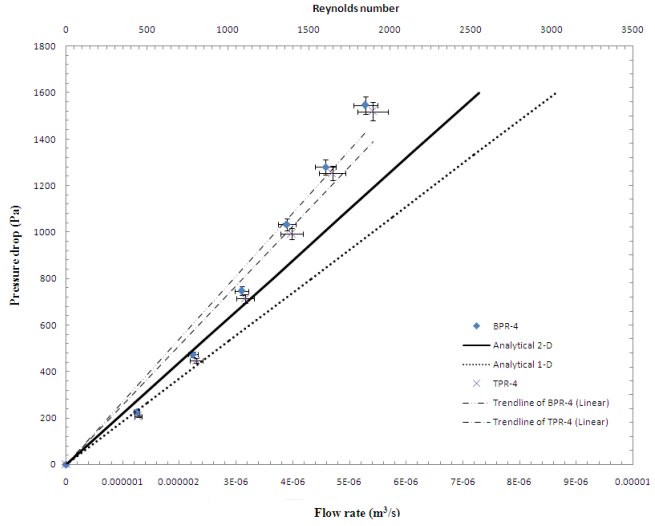

Figure 8. Pressure drop Vs. Flow rate for channel with 1mm height, 4mm width

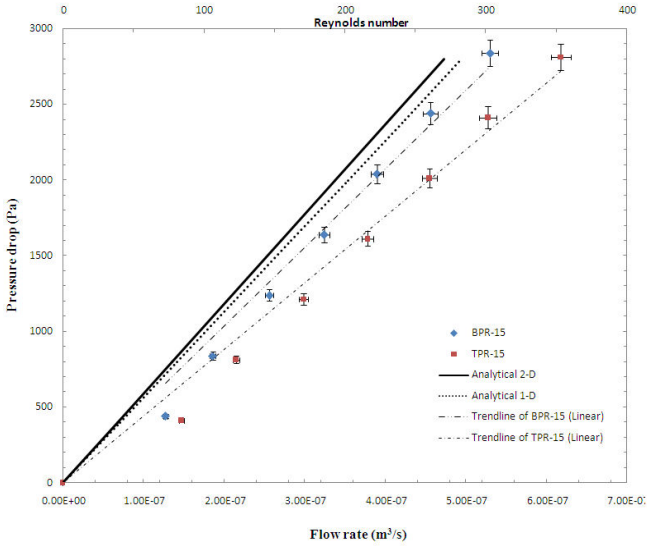

Figure 7. Pressure drop Vs. Flow rate for channel with 0.25 mm height, 4mm width

that the effect of slip is higher for hydrophobized textile channel (TPR-15) compared to the uncoated channel wall (BPR-15). This finding shows the effect of contact angle and surface wettability on drag reduction in microchannels.

Furthermore, to examine the effect of channel wettability (and accordingly the contact angle), a new dimensionless parameter can be defined as follows:

$$\Phi = \frac{Q_{TPR} - Q_{BPR}}{Q_{BPR}} \qquad (14)$$

Q_{TPR} is the flow rate of the PMMA fabricated channel with attached hydrophobized textile. Q_{BPR} refers to the flow rate of

the channel with bare PMMA surfaces. This parameter shows the increase in flow rate due to slip and consequently the invalidity of no-slip BC for modified channel surfaces. Its variation for these microchannels is illustrated in Fig.9.

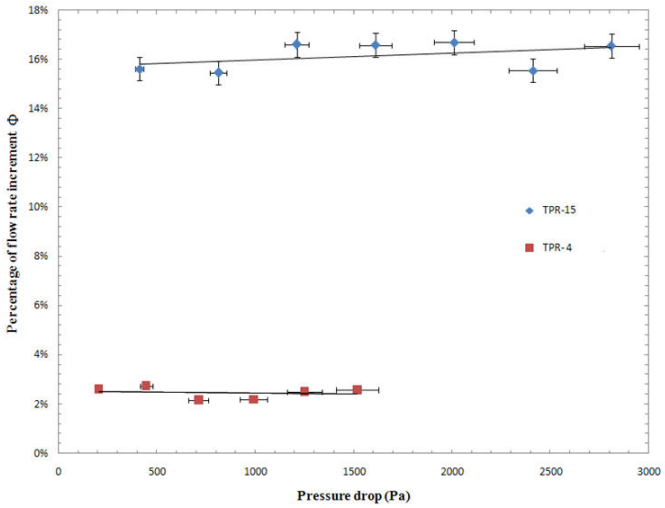

Figure 9. Comparison of percentage of flow rate increscent

From Fig.9, it can be concluded that the flow rate increases by increasing wettability of the surface (increasing static CA angle and minimizing CA hysteresis). For the channel with 1mm height, the flow rate has increased by about 2.5% while it is 16% higher for 0.25 mm channel height. It also amplifies the effect of channel height on the drag reduction (decreasing the pressure drop). As the channel height is decreased to about one-fourth, under the same conditions, the flow rate increases more than 6 times. These results highlight the importance of wettability conditions of the surface in smaller domains since in that case the channel height would be comparable to slip length.

CONCLUSION

In this study, the effects of two important parameters have been evaluated for pressure driven liquid flows in microchannel analytically and experimentally. These parameters are wettability conditions of microchannel surfaces and the aspect ratio of rectangular microchannels. Contact angles which are representative of surface wettability were measured for both bare and attached hydrophobized-textile PMMA surfaces as 54° and 122° respectively. The aspect ratio was varied from 4 to 16. While the width of the channel remains constant, its height was reduced from 1000 to 250 microns. For small aspect ratio, the channel was considered to have a rectangular cross-section, instead of being two parallel plates. A two-dimensional solution based on dual finite series was obtained and extended to the case of a constant slip velocity at the bottom wall. However, for large aspect ratio, a general equation was obtained which is capable of accounting different values of slip lengths for both upper and lower channel walls. All these analytical formulas were written in MATLAB code to better compare with experimental results. Firstly, it was found out that for low aspect ratio microchannels, the result obtained using analytical rectangular 2-D model agrees reasonably well with experimental results as compared to 1-D prediction. For high aspect ratio microchannels, both theoretical models predict the same trend. In addition, experimental results showed that surface wettability affect the pressure drop greatly. The flow rate is higher for the same pressure drop in laminar regime. These findings indicate the importance of increasing slip length in microchannels due to its possibility in reducing pressure drop, or equivalently increasing flow rate at the same pressure difference range.

REFERENCES

[1] Kandlikar, S., et al., *Heat transfer and fluid flow in minichannels and microchannels*. 2006: Elsevier Science Ltd.

[2] Nguyen, N. and S. Wereley, *Fundamentals and applications of microfluidics*. 2002: Artech House Publishers.

[3] Lauga, E., M. Brenner, and H. Stone, *Microfluidics: The no-slip boundary condition Handbook of Experimental Fluid Dynamics, C. Tropea, A. Yarin, JF Foss*. 2007, Springer.

[4] Schnell, E., *Slippage of water over nonwettable surfaces*. Journal of applied physics, 1956. **27**(10): p. 1149-1152.

[5] Churaev, N., V. Sobolev, and A. Somov, *Slippage of liquids over lyophobic solid surfaces.* Journal of Colloid and Interface Science, 1984. **97**(2): p. 574-581.

[6] Cheng, J. and N. Giordano, *Fluid flow through nanometer-scale channels.* Physical Review E, 2002. **65**(3): p. 31206.

[7] Choi, C., et al., *Effective slip and friction reduction in nanograted superhydrophobic microchannels.* Physics of Fluids, 2006. **18**: p. 087105.

[8] Pit, R., H. Hervet, and L. Leger, *Direct experimental evidence of slip in hexadecane: solid interfaces.* Physical review letters, 2000. **85**(5): p. 980-983.

[9] Tretheway, D. and C. Meinhart, *Apparent fluid slip at hydrophobic microchannel walls.* Physics of Fluids, 2002. **14**: p. L9.

[10] Joseph, P., et al., *Slippage of water past superhydrophobic carbon nanotube forests in microchannels.* Physical review letters, 2006. **97**(15): p. 156104.

[11] Wenzel, R., *Resistance of solid surfaces to wetting by water.* Industrial & Engineering Chemistry, 1936. **28**(8): p. 988-994.

[12] Cassie, A.B.D. and S. Baxter, *Wettability of porous surfaces.* Transactions of the Faraday Society, 1944. **40**: p. 546-551.

[13] Watanabe, K., Y. Udagawa, and H. Udagawa, *Drag reduction of Newtonian fluid in a circular pipe with a*

highly water-repellent wall. Journal of Fluid Mechanics, 1999. **381**: p. 225-238.

[14] J. Ou, B.P. and J.P. Rothstein, *Laminar Drag Reduction in Microchannels Using Ultrahydrophobic Surfaces.* Physics of Fluids, 2004(December). **16**(n. 12): p. 4635-4643.

[15] Shah, R. and A. London, *Laminar Flow Forced Convection in Ducts, Academic Press, New York, 1978.* book, 1978.

[16] Bhushan, B., M. Nosonovsky, and Y.C. Jung, *Lotus Effect: Roughness-Induced Superhydrophobic Surfaces*. 2008. p. 995-1072.

[17] Gao, L. and T.J. McCarthy, *"Artificial Lotus Leaf" Prepared Using a 1945 Patent and a Commercial Textile.* Langmuir, 2006. **22**(14): p. 5998-6000.